

IZO deposited by PLD on flexible substrate for organic heterostructures

M. Socol¹ · N. Preda¹ · A. Stanculescu¹ · C. Breazu¹ · C. Florica¹ · O. Rasoga¹ · F. Stanculescu² · G. Socol³

Received: 26 October 2016 / Accepted: 20 April 2017 / Published online: 25 April 2017
© Springer-Verlag Berlin Heidelberg 2017

Abstract In:ZnO (IZO) thin films were deposited on flexible plastic substrates by pulsed laser deposition (PLD) method. The obtained layers present adequate optical and electrical properties competitive with those based on indium tin oxide (ITO). The figure of merit ($9 \times 10^{-3} \Omega^{-1}$) calculated for IZO layers demonstrates that high quality coatings can be prepared by this deposition technique. A thermal annealing (150 °C for 1 h) or an oxygen plasma etching (6 mbar for 10 min.) were applied to the IZO layers to evaluate the influence of these treatments on the properties of the transparent coatings. Using vacuum evaporation, organic heterostructures based on copper phthalocyanine (CuPc) and 3,4,9,10-perylenetetracarboxylic dianhydride (PTCDA) were deposited on the untreated and treated IZO layers. The optical and electrical properties of the heterostructures were investigated by UV–Vis, FTIR and current–voltage (I – V) measurements. For the heterostructure fabricated on IZO treated in oxygen plasma, an improvement in the current value with at least one order of magnitude was evidenced in the I – V characteristics recorded in dark conditions. Also, an increase in the current value for the heterostructure deposited on

untreated IZO layer can be achieved by adding an organic layer such as tris-8-hydroxyquinoline aluminium (Alq₃).

1 Introduction

In the last years, the flexible electronic was a provocation for the researchers, the possibility to make displays that can be bend or roll up representing a new target in the electronic field.

The transparent conductive oxide (TCO) electrodes which are required in the fabrication of the optoelectronic devices should meet some requirements as good optical transmission and adequate electrical properties. The most widely used TCO electrode is ITO, despite the high cost implied in its production. ZnO is another TCO which has comparative properties with ITO. This oxide presents a high thermal stability and involves lower production costs. Moreover, adding In₂O₃, its conductivity can be improved. Thus, have been obtained IZO thin films with low resistivity, high carrier density, good electrical mobility and high transparency in the visible region of the solar spectrum [1–4]. Also, IZO electrode presents “n” conduction type and a large work function (around ~5.2 eV [5]). This TCO electrode can be deposited by various techniques such as: spin-coating from sol–gel [2, 6], radio-frequency sputtering [7, 8] or pulsed laser deposition (PLD) [9–11]).

The PLD is a versatile deposition method which assures the stoichiometric transfer of the materials, resulting high quality thin films [10]. Also, because the PLD does not involve higher processing temperatures it can be applied in the deposition of films on plastic substrates.

Compatible with the flexible substrates are the organic materials because they can be deposited at low

The authors M. Socol and C. Breazu contributed equally to this work.

✉ M. Socol
marcela.socol@infim.ro

¹ National Institute of Material Physics, 405A Atomistilor Street, PO Box MG-7, 077125 Bucharest-Magurele, Romania

² Faculty of Physics, University of Bucharest, 405 Atomistilor Street, PO Box MG-11, 077125 Bucharest-Magurele, Romania

³ National Institute for Lasers, Plasma and Radiation Physics, 409 Atomistilor Street, PO Box MG-36, 077125 Bucharest-Magurele, Romania

temperatures. The main applications of these organic compounds are organic photovoltaic-cells OPV [12, 13], organic light emitting devices-OLEDs [14, 15] and organic thin film transistors-OTFT [16, 17]. The polyethylene terephthalate (PET) [1, 11, 18], polyethylene naphthalate (PEN) [19, 20] and biaxially-oriented polyethylene terephthalate (Mylar) [19, 21] are the most used flexible plastic substrates. Additionally, for the organic films deposition (on different substrates or on large area) can be used with different techniques which do not use expensive set-ups.

In the device applications, the optical and electrical properties of the heterostructures based on organic films play an important role. The interest for the investigation of the interfaces between the organic layer and the TCO electrode is justified by the charge carrier transport properties of the organic material which are comparable with those of the wide-gap inorganic semiconductors [22].

Metal phthalocyanines are planar conjugated aromatic macro cycles featured by an absorption in the ultraviolet and visible range of the solar spectrum. Due to the strong Q-band absorption (600–800) nm, such compounds are promising building blocks for optoelectronic applications. Also, these organic small molecules are used in the therapy of cancer, infectious or neurodegenerative diseases [23]. One of the most investigated metal phthalocyanine is CuPc, a p type semiconductor having the mobility $\mu_p = 1.1 \times 10^{-2} \text{ cm}^2 \text{ V}^{-1} \text{ s}^{-1}$ and the dark conductivity $\sigma_p = 4 \times 10^{-8} \text{ } \Omega^{-1} \text{ cm}^{-1}$ [24]. Usually, CuPc is deposited in thin film form by vacuum evaporation [23, 25, 26]. PTCDA is another promising organic compound that can be easily deposited on different substrates due to its planar molecule [27, 28]. Also, PTCDA is characterised by an absorption in UV and visible domain [29] which makes it suitable for integration in OPV architectures. Alq₃ is an organic that is often used in OPVs and OLEDs, sometime only as a buffer layer for improving the device stability [30]. The above-mentioned materials can be used to obtain organic heterostructures (with a large absorption domain) on IZO flexible substrate instead of commercially ITO.

For technological devices, the stability of the layers in different conditions is a very important factor. Thus, the properties of TCO substrates subjected to different treatments were studied for observing their influence on the performances of the layers [8, 31, 32].

Although, some papers report on the use of IZO films as TCO electrode in OLEDs and OPVs devices [5–7, 33, 34], in the case of IZO films deposited on flexible substrates, the studies were principally focused on their application in OLEDs [7, 34].

In this context, our study presents novel results on the deposition by PLD technique of IZO layers on PET flexible substrate for replacing ITO in the OPV applications.

Furthermore, the influence of treatments such as thermal annealing or oxygen plasma etching on the properties of IZO films was investigated to evidence the way in which can be improved by the electrical properties of the organic heterostructures fabricated on this TCO electrode.

2 Experimental

IZO films were obtained by PLD using a KrF* laser source ($\lambda = 248 \text{ nm}$, $\tau_{\text{FWHM}} = 25 \text{ ns}$, model COMPexPro 205, Lambda Physics-Coherent) in an oxygen atmosphere (1 Pa). IZO targets with atomic In concentration, In/(In + Zn), of 70% were prepared by mixing In₂O₃ (99.9% purity, Aldrich) and ZnO (99.99% purity, Aldrich) powders in a planetary ball mill (model Retsch S 100). The ground powder was pressed at 5 MPa and sintered at 1100 °C in air for 12 h to obtain compact pellets [35].

In the experiments, the following deposition parameters were used: 2 J/cm² laser fluence onto the surface of the target, 4000 applied pulses, 10 Hz repetition rate and 8 cm target–substrate distance. The depositions were made on amorphous-PET (from Goodfellow), at room temperature, without any heating of the substrates. Before deposition, the substrates were cleaned with ethanol and deionised water for 15 min into an ultrasonic bath and then dried with high purity nitrogen.

The obtained IZO/PET layers were treated using an annealing process (IZO-TA) or an oxygen plasma etching process (IZO-OP) to observe the influence of these treatments on the properties of the organic heterostructures deposited on IZO. The resistivity of the IZO layers was measured before and after treatments. The annealing (TA) was made at 70 °C for 1 h into Binder Microbiological Incubator. In literature was reported that the annealing of the TCO coatings can improve the performances of the layers, the resistivity being modified by changing the defect concentration of the films [8]. The oxygen plasma etching (OP) was performed at 0.6 mbar for 10 min into Electronic Diener Plasma-Surface-Technology, Pico Model equipment. In the case of ITO substrates was found that the OP treatment can increase the work function by removing the surface carbon contamination, in this way the emission efficiency of OLED's being enhanced [31]. Also, for aluminium zinc oxide (AZO) was observed that the OP treatment improves the electrical properties of the organic heterostructures obtained on it due to the increase in the work function [32].

The organic active layers (CuPc, PTCDA and Alq₃ from Aldrich) were obtained by vacuum evaporation using an Alcatel system with turbo molecular pump. In the References [9, 31] are given details about this deposition technique. Heterostructures with two or three layers were

prepared on IZO/PET substrates by a successive deposition of CuPc, PTCDA and Alq₃. Also, organic films were deposited on glass and silicon for UV–Vis and FTIR measurements. Heterostructures with three layers were made on IZO untreated (IZO-UN) to investigate the way in which an additional Alq₃ layer affects the electrical properties of the structure. For comparison purpose, CuPc/PTCDA heterostructure was also deposited on ITO. In the deposition chamber, the pressure was varied between 1×10^{-5} and 7.8×10^{-6} mbar. The evaporation temperature was monitored by a thermocouple situated at the bottom of the crucible containing the organic material and was between (263–273) °C for CuPc, (243–252) °C for PTCDA and (218–228) °C for Alq₃.

The back electrode (aluminium—Al) was obtained by vacuum evaporation, the working condition being the following: a pressure of 10^{-4} Pa in the chamber and a deposition rate of 4 Å/s. The thickness of the metallic contact (80 nm) was determined during the deposition process, using a quartz crystal-based monitoring system. The following organic heterostructures, TCO/organic1/organic2/Al or TCO/organic1/organic2/organic3/Al were fabricated.

The structural properties of the IZO samples were analyzed by X-ray diffraction (XRD) with a monochromatised Cu $K_{\alpha 1}$ radiation ($\lambda = 1.5406$ Å) of a diffractometer model Bruker D8 Advance, using 0.6 mm divergent slit. The patterns were collected in the range 20–80° (2θ) range, using a step size of 0.02° and a scan speed of 1 s per step. The thickness of the IZO films (as average media between the values obtained from three different measurements) was evaluated using an Ambios Technology XP 100 profilometer.

The morphology of the layers was investigated using a Zeiss EVO 50XVP scanning electron microscope (SEM) and an atomic force microscope (AFM) from Nanonics (Multiview 4000) working in phase feedback. All the AFM images were recorded on $10 \times 10 \mu\text{m}^2$ areas using a tip with 10 nm in diameter, 37.5 kHz frequency and 1800 quality factor. The AFM parameters were determined before and after IZO treatments.

The optical properties of the layers were examined by measuring the transmission spectra in the UV–VIS range, using a Carry 5000 Spectrophotometer. FTIR measurements were performed in the (700–2000) cm^{-1} domain with a SPECTRUM BX II (Perkin Elmer) Spectrometer.

The electrical resistivity of the IZO coatings were measured before and after treatments at room temperature by a Jandel four point probe head coupled with a Keithley 2182A nanovoltmeter and a Keithley 6220 precision current source for the current generation. The I – V characteristics of the fabricated heterostructures were plotted in dark conditions using a Keithley 2400 Source Meter, having a transversal configuration with 2 wires contact geometry.

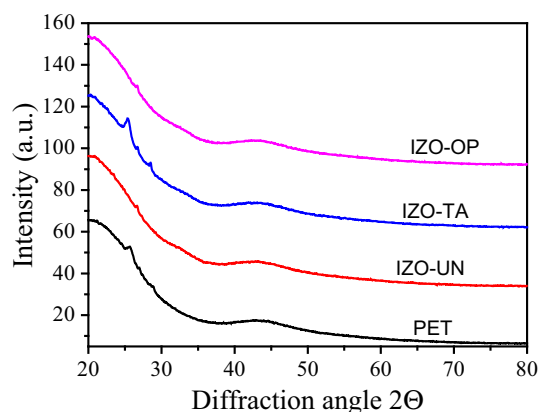


Fig. 1 XRD diagrams of PET (reference), IZO-UN, IZO-TA and IZO-OP samples

3 Results and discussion

The characteristic amorphous structure of IZO films is confirmed by the XRD diagrams (Fig. 1), these presenting only the diffractions lines attributed to PET substrates. The result is in agreement with other previously data related to the IZO layers obtained on PET by PLD, at room temperature, using the same target–substrate distance (8 cm) [35]. Also, the XRD diagrams sustain the hypothesis that no crystallization appears in the IZO layer during the thermal treatment or oxygen plasma etching process. The amorphous structure of the IZO-TA layer is preserved taking into account that in the annealing treatment was used a moderate temperature (70 °C). In literature was reported that the IZO films can remain amorphous even after a thermal treatment at 160 °C for 60 min [36]. Only a shift of the lines characteristic to PET is observed in the case of the IZO-TA layer, probably due to the local stress induced by the annealing process in the PET substrate. A slight curvature of the PET substrate was remarked when it was exposed to the annealing treatment before IZO deposition.

From morphological point of view, the IZO coatings were investigated by SEM (Fig. 2) and AFM (Fig. 3). The interpolated roughness parameters (root mean square—RMS and roughness average—Ra) were determined before and after treatment. IZO-UN presents a topography with irregular grains having a floral aspect (Figs. 2a, 3a). This layer is featured by a small roughness (RMS = 2.4 nm and Ra = 1.8 nm), characteristic for IZO films deposited by PLD [35]. For the IZO-TA coating, an increase in the distance between grains was detected. This can be the effect of the stress induced in the PET substrate during the annealing process. PET bends under the effect of IZO layer and could favour the appearance of small cracks in the film. The hypothesis is also sustained by the increased values of the roughness parameters (RMS = 5.8 nm and

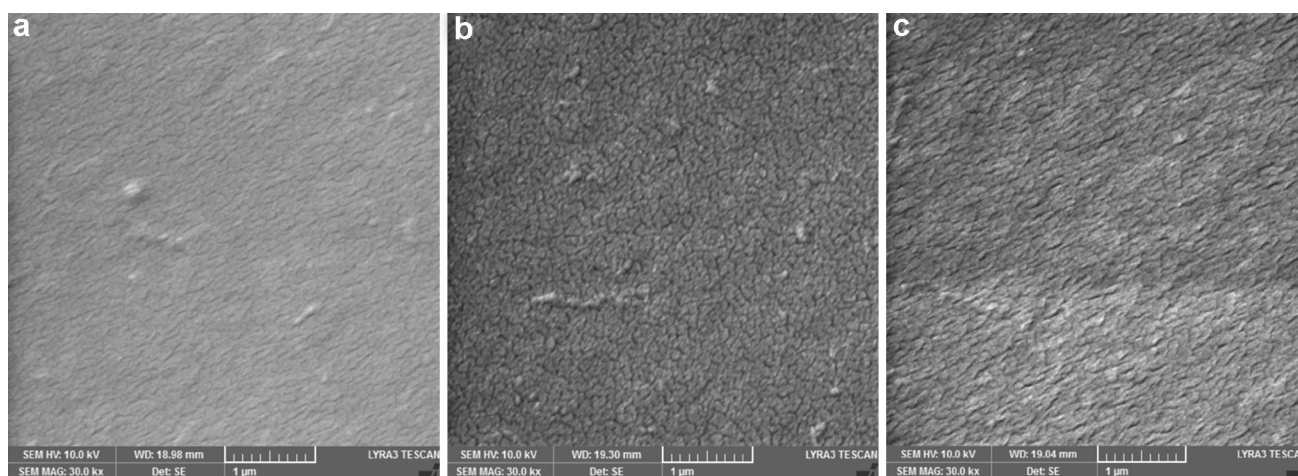


Fig. 2 SEM images of IZO-UN, IZO-TA and IZO-OP layers

$R_a = 4.2$ nm). In the case of IZO-OP coating, a tendency regarding the agglomeration of the grains was evidenced, but without effect in the interpolated roughness values (RMS = 2.4 nm and $R_a = 1.9$ nm). These values are almost identical to those obtained for the IZO-UN film. The SEM images are similar with those reported for IZO films prepared by PLD [9, 10].

The transmittance spectra (Fig. 4a) and the resistivity values of the IZO films deposited by PLD recommend their use in optoelectronic applications. Thus, the as-prepared IZO-UN film has ~ 590 nm in thickness and a resistivity value of about $8.1 \times 10^{-4} \Omega \text{ cm}$, close to that reported for IZO sputtered on PET substrate ($5 \times 10^{-4} \Omega \text{ cm}$) [37]. The treatments do not induce significant changes in the resistivity of the investigated TCO layers, but a slight improvement is observed: $7.3 \times 10^{-4} \Omega \text{ cm}$ for IZO-TA and $6.9 \times 10^{-4} \Omega \text{ cm}$ for IZO-OP. The annealing of the IZO layer can modify the defect concentration in the thin film influencing its electrical properties [38].

All IZO layers present a high transmission in the visible part of the solar spectrum, over 80% (Fig. 4a), which is typical for the IZO films deposited by PLD [10, 35]. The figure of merit (FOM), calculated with Haake formula [39], was $9 \times 10^{-3} \Omega^{-1}$, being similar with the FOM reported for IZO sputtered on glass substrate ($9.2 \times 10^{-3} \Omega^{-1}$) [40]. This parameter estimates quantitatively the quality of the TCO layers with different thickness, transparency and resistivity, its value being usually of $\sim 10^{-4} \Omega^{-1}$. The films characterised by high FOM, must have an increased transparency and a reduced sheet resistance [41]. In our case, the calculated FOM for the IZO layer demonstrates the quality of the deposited films. After applying the treatments mentioned above, the transmittances of the IZO layers (Fig. 4a) were constant ($\sim 80\%$). As was remarked by other authors [42], only a high annealing temperature can induce changes in the structure of IZO films which can

result in an increase of the TCO transmittance value. In our case, it was already noticed that the thermal treatment was made at moderate temperature (70°C). Also, the IZO-OP film is characterised by the same transmission as IZO-TA film, although for another TCO (AZO), an increase in the transmission was reported when the AZO film was exposed to an oxygen plasma etching treatment [32].

To investigate the effect of the treatments applied to the IZO substrate on the properties of the organic heterostructures deposited on it, first, we recorded the UV–Vis spectra of these organic layers deposited on glass (Fig. 4b) for evidencing their characteristic absorption bands. Further, the UV–Vis spectra of the organic layers deposited on IZO-UN, IZO-TA, IZO-OP and ITO (for comparison) were analyzed (Fig. 4c). Thus, the UV–Vis spectra of the heterostructures with two or three organic layers represent a sum of the absorption of the CuPc, PTCDA and Alq₃, covering a large part of the solar spectrum. As it is expected for the phthalocyanine compounds which have an aromatic 18π electrons system with the overlapping orbitals on the central atom, the signature of the CuPc consists a large UV–Vis absorption band. It can be observed that the characteristic B band (“Soret band” between 300 and 450 nm) arising from the direct electronic transition in $d-\pi^*$ orbitals and the Q band (between 600 and 750 nm) with two maxima centred at 626 and 700 nm linked to the $\pi-\pi^*$ transition on the phthalocyaninic macro cycle [43]. The PTCDA exhibits a structured absorption band with two peaks at 357 and 373 nm and a large absorption band with two maxima at 476 and 552 nm. These UV–Vis features of the PTCDA layer are due to the interaction of the π -electron system of the neighbouring planar molecules which in solid state are much closer [44]. The characteristic absorption of Alq₃ is the band with a maximum in the UV domain [29].

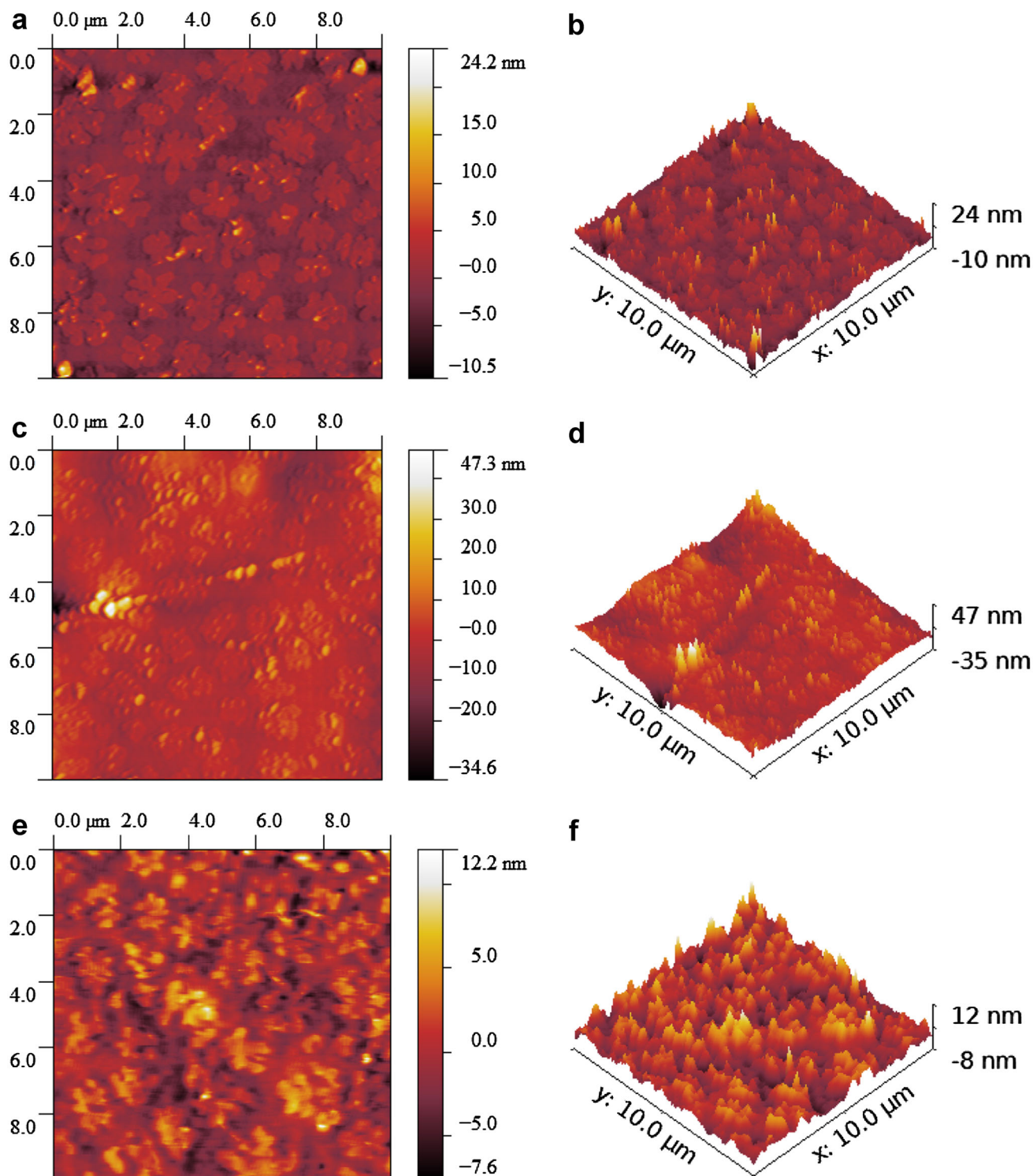


Fig. 3 2D and 3D AFM images of: IZO-UN (a, b), IZO-TA (c, d) and IZO-OP (e, f) layers

The FTIR spectra of the CuPc, PTCDA and Alq₃ thin films (Fig. 5) shows the fingerprint vibrations of the chromophoric groups contained in these organic materials. The FTIR spectrum of CuPc film discloses the peak characteristic to C–H bonds non-planar deformation of benzene

ring at 725 cm⁻¹ [45] and the C–H bonds non-planar vibrations, responsible for the medium peak from 771 cm⁻¹. The peaks from 1065, 1089, 1121, 1166, 1286, 1331, 1424, 1509 cm⁻¹ are attributed to the tetrapyrrolic macro cycle and porphyrin ring system in plane bending

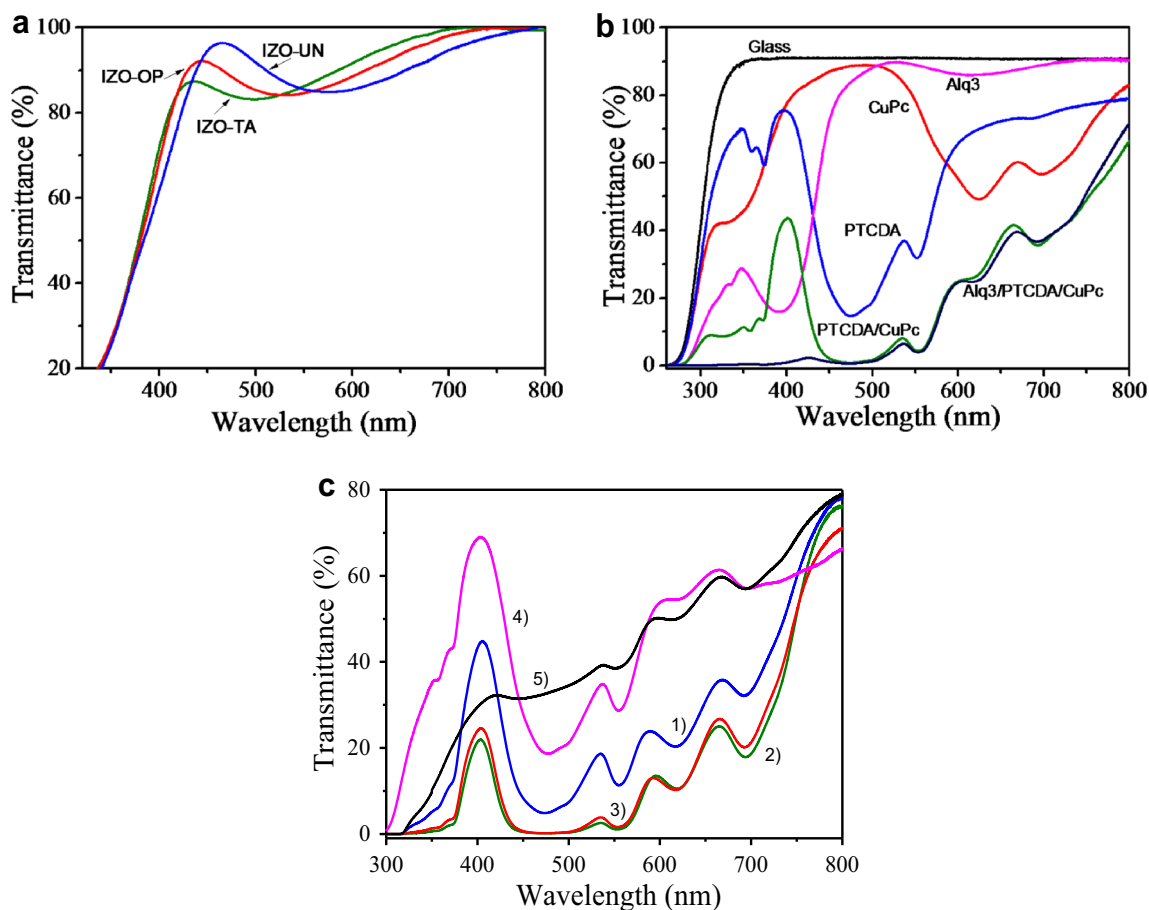


Fig. 4 UV-Vis spectra of **a** IZO layers; **b** organic thin films deposited on glass substrate; **c** organic thin films deposited on IZO and ITO substrate (1-PTCDA/CuPc/IZO-UN, 2-PTCDA/CuPc/IZO-TA, 3-PTCDA/CuPc/IZO-OP, 4-PTCDA/CuPc-ITO and 5-Alq₃/PTCDA/CuPc-IZO-UN)

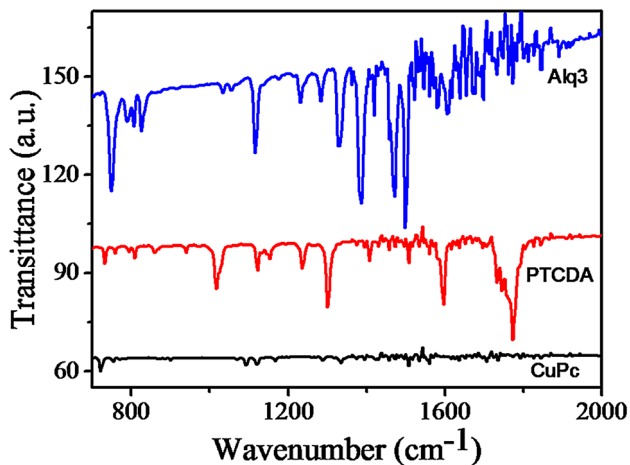


Fig. 5 FTIR spectra of CuPc, PTCDA and Alq₃ films

and stretching [46], the peak from 1333 cm⁻¹ is associated to C–C stretching in isoindole, and the peaks from 1166 and 1828 cm⁻¹ are linked to in-plane stretching of the C–N in isoindole. The band from 1474 cm⁻¹ is due to the C–C benzene ring skeletal stretching [45]. In the FTIR spectrum

of PTCDA film, the following peaks can be identified and attributed: 1020 and 1122 cm⁻¹ to C–O stretching, 1153 cm⁻¹ to asymmetric C–O–C stretching, 1302 and 1408 cm⁻¹ to C–H deformation, 1614 cm⁻¹ to C=O stretching and 1755 cm⁻¹ to carbonyl group [47]. The FTIR spectrum of Alq₃ exhibits the vibrations at 750, 826, 1116, 1228, 1286, 1335, 1384, 1468, 1501, 1577 and 1605 cm⁻¹, which are attributed to C–H wagging, C–H bend, ring stretching, C=N stretching, C=O stretching, respectively [48].

Taking into account that in the FTIR spectra are identified the characteristic vibrations of the investigated organic materials, we can conclude that no significant changes occur in the chemical structure of the deposited layers during the evaporation process.

The *I*–*V* characteristics recorded in dark conditions of the organic heterostructures obtained on untreated and treated IZO deposited on flexible substrates are presented in Fig. 6a. All the heterostructures fabricated on IZO show a near linear behaviour when they were forward biased. The *I*–*V* characteristics show that the applied treatments improve the charge carrier transport in the investigated

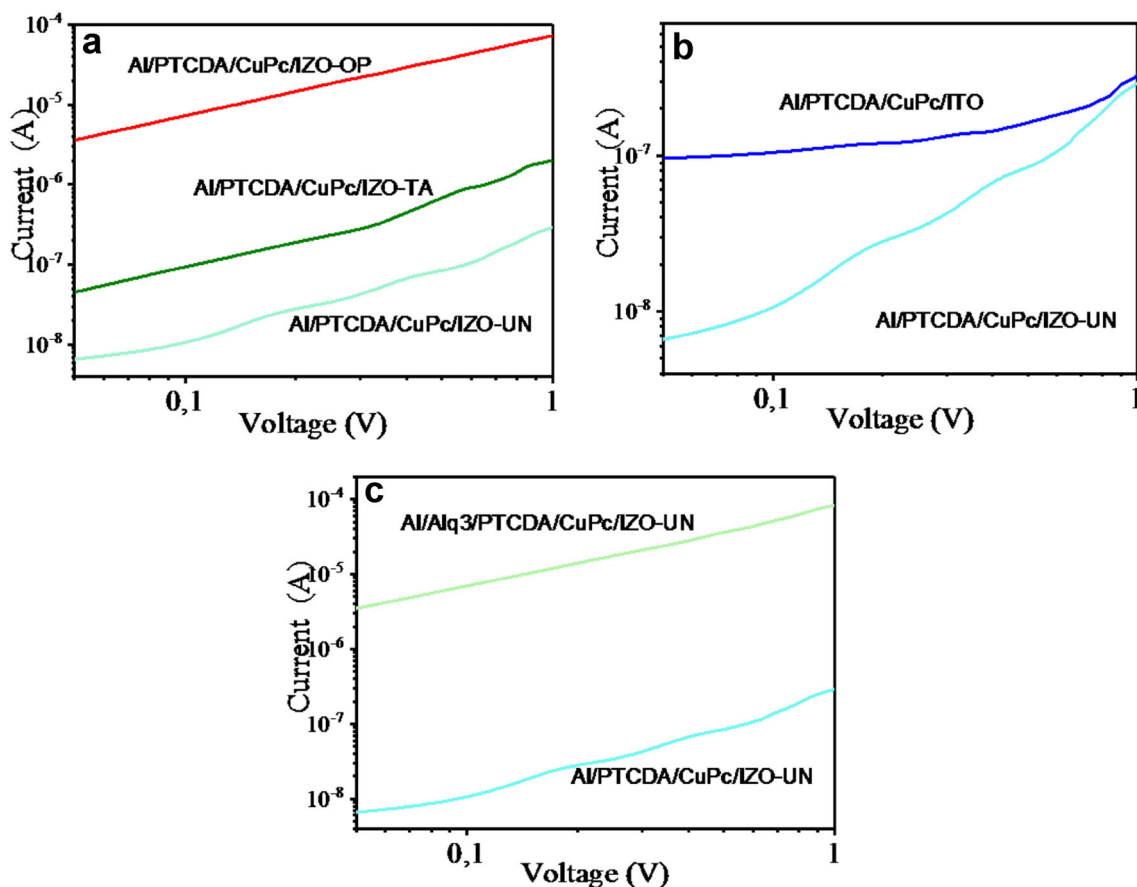


Fig. 6 *I*-*V* characteristics **a** of the prepared organic heterostructures; **b** comparative between PTCDA/CuPc heterostructures on IZO-UN and ITO; **c** comparative PTCDA/CuPc heterostructures on IZO-UN with and without Alq₃ additional layer

organic heterostructures, leading to an increase in the current value of the IZO-OP/CuPc/PTCDA/Al and IZO-TA/CuPc/PTCDA/Al structures in comparison with that of IZO-UN/CuPc/PTCDA/Al structure. The highest current value, 7×10^{-5} A, was obtained for the heterostructures deposited on IZO-OP, this value being comparable with those reported in the case of organic heterostructures based on poly(3-hexylthiophene) and [6]-phenyl C61 butyric acid methyl ester [36] and on pentacene and C60 [49]. It has to be mentioned that these organic heterostructures were also prepared on IZO, but the transparent electrode was deposited on glass substrate. In our case, the increase in the current value was probably due to the lowering of the energetic barrier between IZO and CuPc as a result of the modification generated by the oxygen plasma treatment in the IZO work function. This assumption is in accord with other reported results [31, 32]. Also, in the case of the heterostructure fabricated on IZO-TA, an improvement in the current value (1.9×10^{-6} A) was observed in comparison with that recorded on IZO-UN (2.9×10^{-7} A) (Fig. 6a). This improvement can be based on the change induced by the thermal treatment in the IZO defect

concentration [38]. The defect states can affect the conduction of the IZO layer by reducing the number of the charge carrier through a trapping process.

For comparison, the behaviour of the heterostructure with two organic layers (CuPc and PTCDA) deposited on ITO is also presented (Fig. 6b). This is different from those observed for the heterostructures deposited on IZO. Practically, the heterostructure is featured by a constant current (3.2×10^{-7} A), for voltage <1 V. At 1 V, the current value is close to that obtained in the heterostructure with two organic layers on IZO-UN. From theoretical point of view the alignment of the energetic bands is more favourable in the case of IZO due to its work function (~ 5.2 eV).

A supplementary Alq₃ layer improves the electrical properties of the CuPc/PTCDA heterostructures deposited on IZO-UN, the current value increases from 2.9×10^{-7} to 8.3×10^{-5} A. Thus, an Alq₃ layer can influence the electrical properties of the IZO-UN/CuPc/PTCDA/Al structure by reducing the probability of the short circuit appearance at the deposition of the metallic contact [30].

4 Conclusions

IZO layers characterised by low resistivity, high transmittance and high FOM can be obtained by PLD on flexible PET substrate. The films are smooth (RMS = 2.4 nm) presenting a morphology characteristic to this deposition method. The IZO films were exposed to a thermal annealing or to an oxygen plasma etching process. After these treatments, the IZO layers preserve the optical properties of the initial deposited material, but an improvement in its resistivity was evidenced. The UV–Vis spectra of the organic heterostructures obtained by vacuum evaporation on IZO cover a large domain in the visible part of the solar spectrum. FTIR measurements confirm that no changes appear in the chemical structure of the evaporated CuPc, PTCDA and Alq₃. An improvement with more than one order of magnitude in the current value was observed for the structure with two organic layer deposited on IZO-OP. The organic heterostructures prepared on IZO and ITO present comparable values for the current at 1 V. Also, the electrical properties of the investigated heterostructures deposited on IZO-UN can be improved by adding a supplementary Alq₃ layer. Based on the optical and electrical properties of the organic heterostructures prepared on IZO, this material can be considered as an alternative for TCO in various applications such as OPVs, OLEDs or OFETs.

Acknowledgements This research was financially supported by the Romanian Ministry of Education and Research through National Core Founding Program, contract PN16-480102, by Bilateral contract no. 783/2014 and from contract PN-II-ID-PCE-2012-4-0467.

REFERENCES

- M. Girtan, M. Kompitsas, R. Mallet, I. Fasaki, *Eur. Phys. J. Appl. Phys.* **51**, 33212 (2010)
- M. Girtan, M. Socol, B. Pattier, M. Sylla, A. Stanculescu, *Thin Solid Films* **519**, 573 (2010)
- R. Bel-Hadj-Tahar, A.B. Mohamed, *New J. Glass Ceram.* **4**, 55 (2014)
- K. Ellmer, R. Mientus, *Thin Solid Films* **516**, 4620 (2008)
- J. Cui, A. Wang, N.L. Edleman, J. Ni, P. Lee, N.R. Armstrong, T.J. Marks, *Adv. Mater.* **13**, 1476 (2001)
- A.K.K. Kyaw, Y. Wang, D.W. Zhao, Z.H. Huang, X.T. Zeng, X.W. Sun, *Phys. Status Solidi A* **208**, 2635 (2011)
- J.-H. Bae, J.-M. Moon, J.-W. Kang, H.-D. Park, J.-J. Kim, W.J. Cho, H.-K. Kim, *J. Electrochem. Soc.* **154**, J81 (2007)
- Y.L. Li, H.N. Chao, S.R. Min, S.K. Lim, C.W. Chung, *J. Ind. Eng. Chem.* **13**, 777 (2007)
- P.-Y. Kim, J.-Y. Lee, H.-Y. Lee, S.-J. Lee, N.-I. Cho, *J. Korean Phys. Soc.* **53**, 207 (2008)
- S. Chirakkara, K.K. Nanda, S.B. Krupanidhi, *Thin Solid Films* **519**, 3647 (2011)
- M. Dosmailov, L.N. Leonat, J. Patek, D. Roth, P. Bauer, M.C. Scharber, N.S. Sariciftci, J.D. Pedarnig, *Thin Solid Films* **591**, 97 (2015)
- L. Lucera, F. Machui, P. Kubis, H.D. Schmidt, J. Adams, S. Strohm, T. Ahmad, K. Forberich, H.-J. Egelhaaf, C.J. Brabec, *Energy Environ. Sci.* **9**, 89 (2016)
- L.K. Jagadamma, M. Al-Senani, A. El-Labban, I. Gereige, G.O. Ngongang Ndjawa, J.C.D. Faria, T. Kim, K. Zhao, F. Cruciani, D.H. Anjum, M.A. McLachlan, P.M. Beaujuge, A. Amassian, *Adv. Energy Mater.* **5**, 1500204 (2015)
- H.-Y. Xiang, Y.-Q. Li, L. Zhou, H.-J. Xie, C. Li, Q.-D. Ou, L.-S. Chen, C.-S. Lee, S.-T. Lee, J.-X. Tang, *ACS Nano* **9**, 7553 (2015)
- E. Kim, H. Cho, K. Kim, T.-W. Koh, J. Chung, J. Lee, Y.K. Park, S. Yoo, *Adv. Mater.* **27**, 1624 (2015)
- S. Sung, S. Park, W.-J. Lee, J. Son, C.-H. Kim, Y. Kim, D.Y. Noh, M.-H. Yoon, A.C.S. Appl. Mater. Interfaces **7**, 7456 (2015)
- G. Li, Q. Li, Y. Jin, Y. Zhao, X. Xiao, K. Jiang, J. Wang, S. Fan, *Nanoscale* **7**, 17693 (2015)
- N. Sun, G. Fang, P. Qin, Q. Zheng, M. Wang, X. Fan, F. Cheng, J. Wan, X. Zhao, J. Liu, D.L. Carroll, J. Ye, *J. Phys. D Appl. Phys.* **43**, 445101 (2010)
- A. Stanculescu, M. Socol, G. Socol, I.N. Mihailescu, M. Girtan, N. Preda, A.-M. Albu, F. Stanculescu, *Thin Solid Films* **520**, 1251 (2011)
- D. Karnakis, A. Kearsley, M. Knowles, *J. Laser Micro Nanoeng.* **4**, 218 (2009)
- A.P. Yuen, J.S. Preston, A.-M. Hor, R. Klenkler, E.Q.B. Macabebe, E.E. van Dyk, R.O. Loutfy, *J. Appl. Phys.* **105**, 016105 (2009)
- N. Sai, R. Gearba, A. Dolocan, J.R. Tritsch, W.-L. Chan, J.R. Chelikowsky, K. Leung, X. Zhu, *J. Phys. Chem. Lett.* **3**, 2173 (2012)
- S.S. Mali, D.S. Dalavi, P.N. Bhosale, C.A. Betty, A.K. Chauhancand, P.S. Patil, *RSC Adv.* **2**, 2100 (2012)
- S. Antohe, *J. Optoelectron. Adv. Mater.* **2**, 498 (2000)
- Y. Choe, S.Y. Park, D.W. Park, W. Kim, *Macromol. Res.* **14**, 38 (2006)
- M. Sieryk, O. Dimitriev, T. Doroshenko, K. Grytsenko, O. Kachkovsky, *Proceedings of the International Conference Nanomaterials: Applications and Properties 3*, 01NTF20 (2014)
- J.A. Schuller, S. Karaveli, T. Schiros, K. He, S. Yang, I. Kymissis, J. Shan, R. Zia, *Nat. Nanotechnol.* **8**, 271 (2013)
- H. Huang, S. Chen, X. Gao, W. Chen, A.T. Wee, *ACS Nano* **3**, 3431 (2009)
- A. Stanculescu, F. Stanculescu, L. Tugulea, M. Socol, *Mater. Sci. Forum* **514–516**, 956 (2006)
- L. Cao, Y.-Z. Wang, D.-C. Qi, J.-Q. Zhong, A.T.S. Wee, X.-Y. Gao, *J. Phys. Chem. C* **117**, 25636 (2013)
- F.R. Zhu, in *Organic Light-Emitting Materials and Devices*, ed. by Zhigang-Rick Li, Hong Meng (Taylor & Francis, Boston, 2006), p. 483
- A. Stanculescu, M. Socol, O. Rasoga, I.N. Mihailescu, G. Socol, N. Preda, C. Breazu, F. Stanculescu, *Appl. Surf. Sci.* **302**, 169 (2014)
- Y.-S. Park, K.-H. Choi, H.-K. Kim, *Electrochem. Solid State Lett.* **12**(12), H426 (2009)
- J.-W. Kang, W.-I. Jeong, J.-J. Kim, H.-K. Kim, D.-G. Kim, G.-H. Lee, *Electrochem. Solid State Lett.* **10**(6), J75 (2007)
- G. Socol, M. Socol, N. Stefan, E. Axente, G. Popescu-Pelin, D. Craciun, L. Duta, C.N. Mihailescu, I.N. Mihailescu, A. Stanculescu, D. Visan, A.C. Galca, V. Craciun, *Appl. Surf. Sci.* **260**, 42 (2012)
- H. Cheun, J. Kim, Y. Zhou, Y. Fang, A. Dindar, J. Shim, C. Fuentes-Hernandez, K.H. Sandhage, B. Kippelen, *Opt. Express* **18**, A506 (2010)
- Y. Yan, X.-F. Zhang, Y.-T. Thin Solid Films **532**, 79 (2013)
- D. Kilian, S. Polster, I. Vogeler, M.P.M. Jank, L. Frey, W. Peukert, A.C.S. Appl. Mater. Interfaces **6**, 12245 (2014)
- G. Haacke, *J. Appl. Phys.* **47**, 4086 (1976)

40. H.-J. Kim, K.-W. Seo, Y.-J. Noh, S.-I. Na, A. Sohn, D.-W. Kim, H.-K. Kim, *Sol. Energ. Mater. Sol. Cells* **141**, 194 (2015)
41. Z. Chen, W. Li, R. Li, Y. Zhang, G. Xu, H. Cheng, *Langmuir* **29**, 13836 (2013)
42. G. Gonçalves, E. Elangovan, P. Barquinha, L. Pereira, R. Martins, E. Fortunato, *Thin Solid Films* **515**, 8562 (2007)
43. J. Puigdollers, C. Voz, M. Fonrodona, S. Cheylan, M. Stella, J. Andreu, M. Vetter, R. Alcubilla, *J. Non Cryst. Solids* **352**, 1778 (2006)
44. A. Stanculescu, M. Socol, G. Socol, I.N. Mihailescu, F. Stanculescu, M. Girtan, *Appl. Phys. A* **104**, 921 (2011)
45. S. Sivamalar, J. Shanthi, Pon Kalugasalam. *Int. J. Modern Eng. Res.* **2**, 3032 (2012)
46. M. Ghosh, N. Padma, R. Tewari, A.K. Debnath, *J. Phys. Chem. C* **118**, 691 (2014)
47. M. Pandey, G.M. Joshi, K. Deshmukh, N.N. Ghosh, N.A.N. Raj, *J. Phys. Chem. Sol.* **80**, 52 (2015)
48. Y. Sakurai, Y. Hosoi, H. Ishii, Y. Ouchi, *J. Appl. Phys.* **96**, 5534 (2004)
49. X. Chen, D. Taguchi, T. Manaka, M. Iwamoto, *Appl. Phys. Lett.* **104**, 013306 (2014)